JOURNAL OF SOLID STATE CHEMISTRY 89, 282–291 (1990)

Structure Determination of β- and γ-$BaAlF_5$ by X-Ray and Neutron Powder Diffraction: A Model for the $\alpha \rightarrow \beta \leftrightarrow \gamma$ Transitions

ARMEL LE BAIL, GÉRARD FEREY, AND ANNE-MARIE MERCIER

Laboratoire des Fluorures, URA CNRS 449, Université du Maine, Faculté des Sciences, 72017 Le Mans Cedex, France

ARIEL DE KOZAK AND MAURICE SAMOUËL

Laboratoire de Cristallochimie du solide, URA CNRS 1388, Université Pierre-et-Marie-Curie, Tour N°54, 4 Place Jussieu, 75252 Paris Cedex 05, France

Received March 8, 1990

β-$BaAlF_5$ is monoclinic (space group $P2_1/n$): a = 5.1517(1) Å, b = 19.5666(4) Å, c = 7.5567(2) Å, β = 92.426(1)°, Z = 8. γ-$BaAlF_5$ is monoclinic (space group $P2_1$): a = 5.2584(1) Å, b = 9.7298(2) Å, c = 7.3701(2) Å, β = 90.875(1)°, Z = 4. Both structures are determined ab initio from X-ray powder data; final results are given from neutron powder data refinements (R_I = 0.038, R_P = 0.072, and R_{WP} = 0.087 and R_I = 0.048, R_P = 0.083, and R_{WP} = 0.101 for the β and γ phases, respectively). Like α-$BaAlF_5$, the β and γ phases are built up from isolated infinite $(AlF_5)_n^{2n-}$ chains with AlF_6 octahedra sharing corners in a *cis*-position. Close structural relationships are shown to exist between the Ba–Al cationic subnetwork of: α-$BaAlF_5$ and the CrB-type structure; β-$BaAlF_5$ and the SrAg-type; γ-$BaAlF_5$ and the FeB-type. The polymorphic transitions are proposed to be topotactic and a displacive mechanism is suggested.

Introduction

In 1982, Domesle and Hoppe (*1*) established that $BaAlF_5$ occurs in three polymorphs. They solved the structure of the low temperature form α-$BaAlF_5$, which is isotypic with $BaGaF_5$ (*2*). Their investigations by DTA and quenching proved that the α form transforms irreversibly into β-$BaAlF_5$. The transformation starts slowly at 666°C and is detected at 736°C on the DTA curve (*1*). The reversible transition from β- to γ-$BaAlF_5$ occurs at 789°C. They determined the β and γ unit cells from single crystal data (both monoclinic with the proposed space group $P2_1/m$ or $P2_1$); the poor quality of the crystals prevented the structure determination.

Typically, many phases remain structurally uncharacterized because of systematic twinning and/or fragmentation occurring at transitions. Means to remedy such a situation are extensively developed: X-rays from a synchrotron source for microcrystal, electronic microdiffraction, tunneling microscopy, and powder diffraction. The ability of the last method to solve moderately complex structures with a reasonable accuracy has now been established.

This study makes use of X-ray and neutron powder diffraction to solve and refine the β- and γ-$BaAlF_5$ structures. The deci-

0022-4596/90 $3.00

sion to elucidate these structures originated from our recent reinvestigation of the BaF_2–AlF_3 binary system for which the existence of some phases remains the subject of some controversy.

Experimental

All the syntheses were performed by solid state reaction in sealed gold or platinum tubes, under inert atmosphere (argon). The α phase was obtained from the stoichiometric BaF_2: AlF_3 mixture (15 hr, 600°C); the β phase was prepared from the α phase (3 days, 740°C); the γ phase was obtained when β-$BaAlF_5$ was heated 1 day at 850°C, cooled down to 800°C, stabilized 15 min at this temperature, and then quenched in water.

X-ray powder patterns were recorded on a Siemens D501 diffractometer (Cu$K\alpha$; graphite back-monochromator). A side-loaded sample holder was used to avoid preferred orientation effects occurring when the samples were pressed. Very small amounts of $Ba_3Al_2F_{12}$ (*3*), less than 1% in volume, were always present in various preparations of the α phase; similar amounts of β are found in γ-$BaAlF_5$.

The neutron powder patterns were recorded at the Institut Max von Laue–Paul Langevin on the D2B diffractometer (λ = 1.5945 Å) operating at medium resolution.

Structure Determination of β- and γ-$BaAlF_5$

Domesle and Hoppe (*1*) suggested possible relationships among the cell parameters of the three phases. Particularly, $c_\alpha \approx a_\beta \approx a_\gamma \approx 5$ Å could suggest that the β- and γ-$BaAlF_5$ are composed of isolated infinite $(AlF_5)_n^{2n-}$ *cis*-chains of AlF_6 corner sharing octahedra like in α-$BaAlF_5$ (Fig. 1). This was no help in solving the structures. Classical powder methodology was therefore used: cell-constrained pattern fitting followed by

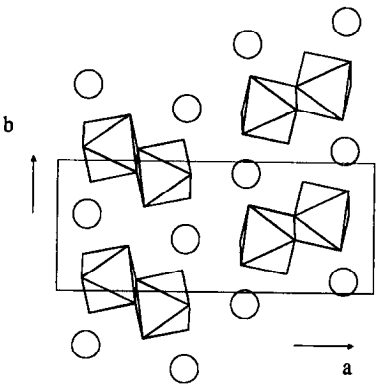

FIG. 1. A [001] projection of the α-$BaAlF_5$ structure.

Patterson or/and direct methods applied on "nonoverlapping reflections" (the criterion for "nonoverlapping" being arbitrarily chosen as the angular position differing by more than one or two counting steps from neighboring reflections). The program used for pattern fitting has been described in Ref (*4*). The proposed space groups $P2_1/m$ and $P2_1$ were thus confirmed for the γ phase while the $P2_1/n$ space group was unambiguous for the β phase.

In both cases, direct methods (option TANG of the SHELX-76 program (*5*)) provided the solution with the heavy atoms in two general positions (using the noncentric space group $P2_1$ for γ-$BaAlF_5$). Ionic scattering factors were taken from the "International Tables for X-ray Crystallography" (*6*). Refinement of the Ba atomic coordinates, using 406 or 366 reflections for the β and the γ phases, respectively, leads to the corresponding R values 0.39, 0.29. The aluminum atoms were then located from a Fourier difference map; their introduction lowered the discrepancy factors to respectively 0.35 and 0.26. It was difficult to go further with the data originating from the pattern fitting. The fluorine atoms were successively located by a laborious procedure alternating Rietveld refinement and Fourier difference syntheses.

TABLE I

CONDITIONS OF STRUCTURE DETERMINATION AND RIETVELD REFINEMENTS

	α	β	γ
Space group:	$P2_12_12_1$	$P2_1/n$	$P2_1$
Z:	4	8	4
X-ray			
2θ range	10–120	5–120	10–122
Step (°2θ)	0.04	0.02	0.04
Number of *hkl*	361	1130	615
hkl used for solving discrepancy factors from pattern fitting		403	366
R_P		0.058	0.071
R_{WP}		0.073	0.088
from Rietveld			
R_I	0.033	0.052	0.054
R_P	0.080	0.084	0.094
R_{WP}	0.099	0.099	0.113
Neutrons			
2θ range	10–147	10–147	10–147
Step (°2θ)	0.05	0.05	0.05
Number of *hkl*	432	1383	728
Number of refined parameters:			
Total	37	66	65
x,y,z,B	28	56	55
Cell parameters			
a(Å)	13.7168(3)	5.1517(1)	5.2584(1)
b(Å)	5.6054(2)	19.5666(4)	9.7298(2)
c(Å)	4.9329(1)	7.5567(2)	7.3701(2)
β(°)		92.426(1)	90.875(1)
V(Å^3)	379.28	761.04	377.03
Profile parameters			
Zeropoint (°2θ)	0.0450(5)	0.0496(5)	0.0582(5)
U	0.098(3)	0.072(2)	0.068(3)
V	−0.176(7)	−0.179(5)	−0.166(6)
W	0.200(3)	0.202(3)	0.196(3)
Eta	0.294(8)	0.292(9)	0.306(9)
Discrepancy factors			
R_I	0.040	0.038	0.048
R_F	0.027	0.023	0.029
R_P	0.084	0.072	0.083
R_{WP}	0.099	0.087	0.101
R_E	0.053	0.050	0.051

Note. R_P and R_{WP} are calculated after background subtraction.

The final results from X-ray data give clearly the crystal chemistry of the β and γ phases. However, both Al and F are quite light elements compared to Ba; this fact, combined with the inherent medium accuracy of the powder method due to overlapping, explained why accuracy of bond lengths was poor in the case of α-$BaAlF_5$. For instance, discrepancies in the Al–F distances using the single crystal results (*1*) reached 0.07 Å. In such a case, neutron diffraction appears necessary to improve the quality of this study.

Refinements from neutron diffraction

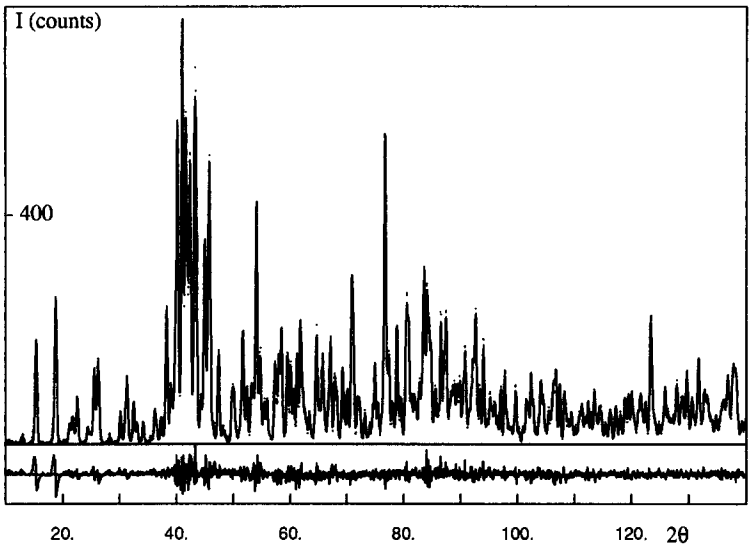

FIG. 2. Observed (···) and calculated (—) neutron patterns of β-$BaAlF_5$. The difference pattern is below at the same scale.

data were made with the DBW3.2S program (*7*, *8*) using a pseudo-Voigt profile shape function. Table I gathers the conditions of the Rietveld refinements and profile fitting procedures. The observed and calculated neutron patterns are shown in Figs. 2 and 3. To save space the Rietveld X-ray final coordinates are not given. Table II compares the single crystal X-ray results (*1*) to the neutron data results. The mean observed

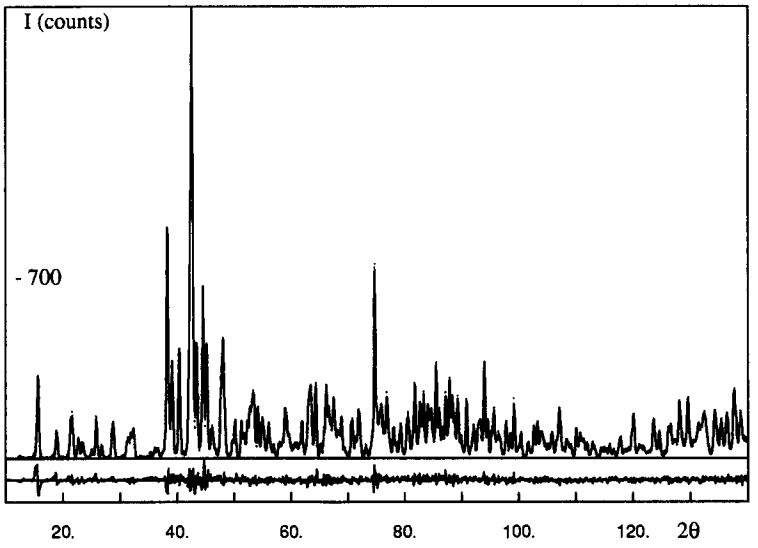

FIG 3. Observed (···) and calculated (—) neutron patterns of γ-$BaAlF_5$. The difference pattern is below at the same scale.

TABLE II

COMPARISON BETWEEN THE ATOMIC COORDINATES ($\times 10^4$) AND THERMAL PARAMETERS OF α-$BaAlF_5$ FROM X-RAY SINGLE CRYSTAL DATA (*1*) (*Beq*) AND POWDER NEUTRON DATA (*B*) (*Italics*)

Atom	*x*	*y*	*z*	*Beq*/*B* (Å^2)
Ba	−938(0)	888(1)	199(1)	0.78(2)
	−943(2)	*905(5)*	*197(4)*	*0.84(4)*
Al	−1650(2)	5971(5)	4367(5)	0.67(7)
	−1652(2)	*5981(7)*	*4362(8)*	*0.75(5)*
F(1)	−2733(4)	1482(10)	8147(12)	1.19(18)
	−2740(2)	*1454(5)*	*8142(5)*	*1.19(5)*
F(2)	−4195(4)	2154(10)	1170(12)	1.23(18)
	−4188(2)	*2151(5)*	*1164(5)*	*1.39(5)*
F(3)	−1055(4)	3354(10)	5497(12)	1.28(18)
	−1041(2)	*3334(5)*	*5496(5)*	*1.23(5)*
F(4)	−796(4)	5991(11)	1570(11)	1.31(18)
	−792(2)	*5997(5)*	*1563(5)*	*1.33(4)*
F(5)	−2490(4)	4122(10)	2251(11)	1.13(17)
	−2489(2)	*4099(5)*	*2258(5)*	*1.09(4)*

discrepancies (as fractions of the *a*, *b*, and *c* parameters) are 0.0006, 0.0014, and 0.0005, respectively (the maxima are 0.0014, 0.0028, and 0.0007, corresponding to 0.019, 0.016, and 0.004 Å, respectively). This establishes the degree of accuracy which can be expected for the β and γ phases (note however, that the number of refined parameters is doubled). Atomic coordinates for the β and γ phases are listed in Tables III and IV. All refinements were made in the isotropic *B* factors approximation. The main interatomic distances are listed in Table V. For α-$BaAlF_5$ the maximum difference with the single crystal results is 0.026 Å for Al–F(*3*); for the mean value, it is <0.01 Å.

Description of the Structures

The three phases can be described using the same few words: the AlF_6 octahedra

TABLE III

β-$BaAlF_5$ ATOMIC COORDINATES ($\times 10^4$) AND THERMAL PARAMETERS FROM POWDER NEUTRON DATA

Atom	*x*	*y*	*z*	*B* (Å^2)
Ba(1)	2820(7)	389(2)	7400(5)	0.89(6)
Ba(2)	2560(7)	2700(2)	4743(5)	0.90(7)
Al(1)	2460(11)	8680(3)	5280(7)	0.79(8)
Al(2)	7676(12)	8925(3)	8495(8)	1.06(8)
F(1)	9456(7)	4002(2)	8494(5)	1.17(6)
F(2)	7470(7)	4830(2)	6195(5)	1.24(6)
F(3)	2134(8)	1983(2)	1826(5)	1.21(6)
F(4)	5056(6)	1142(2)	141(4)	1.34(7)
F(5)	4438(7)	4037(2)	7870(5)	0.98(7)
F(6)	2670(6)	4543(2)	587(5)	1.12(7)
F(7)	584(7)	3389(2)	1469(4)	1.07(6)
F(8)	5226(6)	3841(2)	4567(5)	0.93(6)
F(9)	5420(7)	3446(2)	892(5)	1.36(7)
F(10)	2749(8)	7882(2)	6440(6)	1.52(7)

TABLE IV

γ-$BaAlF_5$ Atomic Coordinates ($\times 10^4$) and Thermal Parameters from Powder Neutron Data

Atom	x	y	z	B (Å^2)
Ba(1)	105(10)	0	8864(7)	1.15(9)
Ba(2)	4871(11)	3472(6)	6389(7)	0.96(8)
Al(1)	101(18)	6266(9)	5701(10)	1.32(12)
Al(2)	5145(13)	7334(8)	8680(8)	0.49(8)
F(1)	2518(9)	464(7)	5324(7)	1.44(9)
F(2)	2519(9)	2536(7)	9442(7)	1.47(10)
F(3)	7654(9)	361(7)	5553(7)	1.18(9)
F(4)	2677(8)	7345(8)	329(7)	1.29(9)
F(5)	387(9)	5110(7)	7553(6)	1.42(8)
F(6)	5064(9)	9165(6)	8419(6)	0.89(8)
F(7)	9916(10)	2619(5)	6009(7)	1.56(9)
F(8)	4485(8)	569(6)	1350(7)	1.51(8)
F(9)	2832(8)	7286(7)	6782(6)	1.40(8)
F(10)	7924(8)	7449(7)	7038(7)	1.44(8)

share corners in *cis*-positions to form isolated chains directed along one axis (Figs. 1, 4, and 5). The Al–F–Al angles show only a little variation, less than would be expected from the systematic increase of the cell parameter in the chain direction from α to γ. In α-$BaAlF_5$, Ba is 12-coordinated in a distorted cuboctahedron (*1*); in the two H.T. phases, the same polyhedron can be recognized only for Ba(2) in β-$BaAlF_5$; however, the twelfth fluorine has moved to a distance longer than 3.6 Å from Ba. Other Ba sites do not clearly correspond to defined polyhedra.

From Figs. 1, 4, and 5, a feature in common between the three phases, which is not immediately apparent (if one excepts the octahedral chains), becomes obvious when the

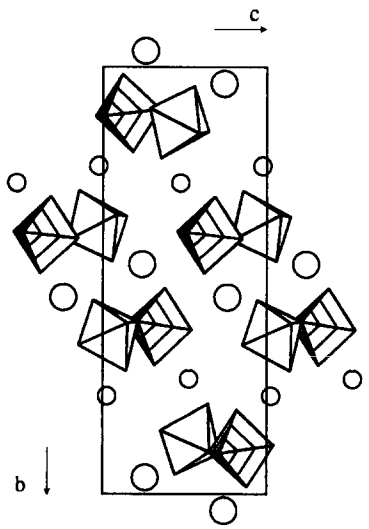

FIG. 4. A [100] projection of the β-$BaAlF_5$ structure. Ba(1) atoms are shown as the largest circles and Al(1)F_6 octahedra are unshaded.

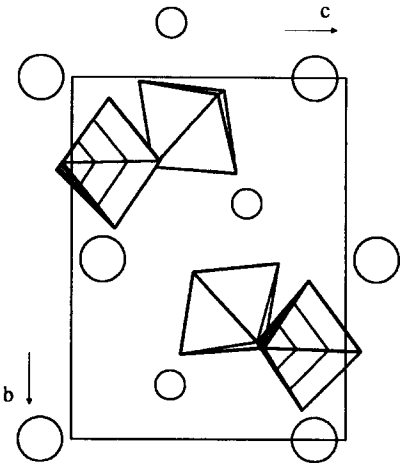

FIG. 5. A [100] projection of the γ-$BaAlF_5$ structure. Ba(1) atoms are shown as the largest circles and Al(1)F_6 octahedra are unshaded.

TABLE V

SELECTED INTERATOMIC DISTANCES (Å) AND ANGLES (°) FOR α [FROM X-RAY (*I*) AND NEUTRON RESULTS], β- AND γ-$BaAlF_5$

α-$BaAlF_5$		β-$BaAlF_5$		γ-$BaAlF_5$	
		AlF_6 octahedra			
X-ray					
Al–F(1)	1.765(6)	Al(1)–F(7)	1.736(7)	Al(1)–F(1)	1.74(1)
Al–F(2)	1.799(6)	Al(1)–F(9)	1.756(7)	Al(1)–F(3)	1.75(1)
Al–F(3)	1.768(6)	Al(1)–F(10)	1.794(7)	Al(1)–F(5)	1.77(1)
Al–F(4)	1.809(6)	Al(1)–F(6)	1.812(7)	Al(1)–F(7)	1.82(1)
Al–F(5)	1.848(6)	Al(1)–F(5)	1.875(7)	Al(1)–F(10)	1.91(1)
Al–F(5)	1.868(6)	Al(1)–F(1)	1.912(7)	Al(1)–F(9)	1.91(1)
{Al–F}	1.809	{Al(1)–F}	1.814	{Al(1)–F}	1.818
Neutrons					
Al–F(1)	1.768(5)	Al(2)–F(4)	1.784(7)	Al(2)–F(8)	1.73(1)
Al–F(2)	1.793(5)	Al(2)–F(2)	1.788(7)	Al(2)–F(4)	1.79(1)
Al–F(3)	1.794(5)	Al(2)–F(8)	1.791(7)	Al(2)–F(6)	1.79(1)
Al–F(4)	1.816(5)	Al(2)–F(3)	1.796(7)	Al(2)–F(9)	1.84(1)
Al–F(5)	1.852(5)	Al(2)–F(1)	1.830(7)	Al(2)–F(2)	1.85(1)
Al–F(5)	1.873(5)	Al(2)–F(5)	1.858(7)	Al(2)–F(10)	1.91(1)
{Al–F}	1.816	{Al(2)–F}	1.808	{Al(2)–F}	1.819
Al–Al	3.564(3)	Al(1)–Al(2)	3.578(8)	Al(1)–Al(2)	3.572(9)
Al–F(5)-Al	146.2(3)	Al(1)–F(1)–Al(2)	145.9(5)	Al(2)–F(9)–Al(1)	144.5(7)
		Al(1)–Al(2)	3.566(7)	Al(1)–Al(2)	3.587(9)
		Al(1)–F(5)–Al(2)	145.6(5)	Al(1)–F(10)–Al(2)	139.5(6)
		Ba environment			
X-ray					
Ba–F(2)	2.624(6)	Ba(1)–F(8)	2.631(6)	Ba(1)–F(5)	2.659(7)
Ba–F(1)	2.682(6)	Ba(1)–F(7)	2.725(6)	Ba(1)–F(6)	2.755(7)
Ba–F(1)	2.683(6)	Ba(1)–F(4)	2.754(6)	Ba(1)–F(3)	2.765(7)
Ba–F(3)	2.704(6)	Ba(1)–F(6)	2.802(6)	Ba(1)–F(4)	2.780(7)
Ba–F(2)	2.715(6)	Ba(1)–F(9)	2.811(6)	Ba(1)–F(6)	2.787(7)
Ba–F(4)	2.833(6)	Ba(1)–F(2)	2.827(6)	Ba(1)–F(2)	2.804(7)
Ba–F(4)	2.862(6)	Ba(1)–F(5)	2.894(6)	Ba(1)–F(1)	2.953(7)
Ba–F(4)	2.945(6)	Ba(1)–F(6)	2.903(6)	Ba(1)–F(8)	2.973(7)
Ba–F(3)	2.959(6)	Ba(1)–F(2)	2.913(6)	Ba(1)–F(10)	3.040(7)
Ba–F(5)	2.972(6)	Ba(1)–F(6)	2.937(6)	Ba(1)–F(2)	3.044(7)
Ba–F(3)	3.098(6)	Ba(1)–F(1)	3.142(6)	Ba(1)–F(4)	3.102(7)
Ba–F(2)	3.407(6)	Ba(1)–F(2)	3.162(6)	Ba(1)–F(7)	3.305(6)
Neutrons				Ba(1)–F(9)	3.38(7)
Ba–F(2)	2.632(4)	Ba(2)–F(3)	2.614(6)	Ba(2)–F(8)	2.653(8)
Ba–F(1)	2.669(4)	Ba(2)–F(8)	2.628(6)	Ba(2)–F(3)	2.671(8)
Ba–F(1)	2.683(4)	Ba(2)–F(4)	2.631(6)	Ba(2)–F(1)	2.700(8)
Ba–F(3)	2.692(4)	Ba(2)–F(9)	2.661(6)	Ba(2)–F(2)	2.740(8)
Ba–F(2)	2.726(4)	Ba(2)–F(3)	2.846(6)	Ba(2)–F(7)	2.745(8)
Ba–F(4)	2.841(4)	Ba(2)–F(10)	2.849(6)	Ba(2)–F(7)	2.798(8)
Ba–F(4)	2.867(4)	Ba(2)–F(10)	2.917(6)	Ba(2)–F(9)	2.888(8)
Ba–F(4)	2.939(4)	Ba(2)–F(7)	3.054(6)	Ba(2)–F(4)	2.936(8)
Ba–F(3)	2.950(4)	Ba(2)–F(7)	3.061(6)	Ba(2)–F(5)	2.983(8)
Ba–F(5)	2.955(4)	Ba(2)–F(10)	3.061(6)	Ba(2)–F(10)	3.069(8)
Ba–F(3)	3.099(4)	Ba(2)–F(3)	3.324(6)	Ba(2)–F(1)	3.269(8)
Ba–F(2)	3.411(4)			Ba(2)–F(5)	3.408(8)
				Ba(2)–F(3)	3.422(9)

TABLE VI

THE SIMILARITIES (CELL PARAMETERS AND ATOMIC COORDINATES) AMONG CrB, SrAg, FeB (DENOTED I) AND α, β, γ-$BaAlF_5$, RESPECTIVELY (DENOTED II), NEGLECTING THE MONOCLINIC DISTORTIONS FOR β AND γ-$BaAlF_5$

CrB	*Cmcm*	*a*I = 2.969	*b*I = 7.858	*c*I = 2.932	*Z* = 4
α-$BaAlF_5$	$P2_12_12_1$	*a*II = 13.717	*b*II = 5.605	*c*II = 4.933	*Z* = 4
		*a*I/*b*II = 0.53	*b*I/*a*II = 0.57	*c*I/*c*II = 0.59	
		*y*I, (*x*II + 1/4)	*x*I, *y*II		*z*I, (*z*II + 1/4)
Cr, Ba		0.146, 0.156	0.000, 0.091		0.250, 0.270
B, Al		0.440, 0.415	0.000, 0.098		0.250, 0.314
		plus three other positions obtained as			
		$-X,-Y,1/2+Z$; $1/2+X,1/2-Y,1/2-Z$; $1/2-X,1/2+Y,-Z$			
SrAg	*Pnma*	*a*I = 16.558	*b*I = 4.788	*c*I = 6.385	*Z* = 8
β-$BaAlF_5$	$P2_1/n$	*a*II = 5.152	*b*II = 19.567	*c*II = 7.557	*Z* = 8
		*a*I/*b*II = 0.85	*b*I/*a*II = 0.93	*c*I/*c*II = 0.84	
		*y*I, *x*II	*x*I, *y*II		*z*I, *z*II
Sr1, Ba1		0.250, 0.256	0.285, 0.270		0.513, 0.474
Sr2, Ba2		0.250, 0.282	0.035, 0.039		0.747, 0.740
Ag1, Al1		0.250, 0.254	0.358, 0.368		0.003, 0.972
Ag2, Al2		0.250, 0.232	0.108, 0.107		0.257, 0.151
		plus three other positions obtained as			
		$-X,-Y,-Z$; $1/2-X,1/2+Y,1/2-Z$; $1/2+X,1/2-Y,1/2+Z$			
FeB	*Pnma*	*a*I = 5.495	*b*I = 2.946	*c*I = 4.053	*Z* = 4
γ-$BaAlF_5$	$P2_1$	*a*II = 5.258	*b*II = 9.730	*c*II = 7.370	*Z* = 4
		*a*I/*b*II = 0.56	*b*I/*a*II = 0.56	*c*I/*c*II = 0.55	
		*y*I,(*x*II + 3/4)	*x*I,(*y*II + 0.32)		*z*I,(*z*II + 1/4)
Fe, Ba1		0.250, 0.263	0.180, 0.167		0.125, 0.111
Fe, Ba2		0.750, 0.739	0.820, 0.820		0.875, 0.864
B, Al1		0.250, 0.265	0.036, 0.053		0.610, 0.618
B, Al2		0.750, 0.760	0.964, 0.947		0.390, 0.320
		plus another position obtained as			
		$1/2-X,1/2+Y,1/2-Z$			

cationic arrangement is examined. From this point of view, the three phases are built up from the same basic structural unit: a monocapped trigonal prism of Ba enclosing an Al. Moreover, in each case, these trigonal prisms share faces to form infinite chains (oriented as the octahedral chains). Then the analogy with some very simple and well known diatomic compounds is evident: the Ba–Al cationic arrangement in the structure of α-$BaAlF_5$ shows only weak deviations from the CrB-type structure (*9*); in the case of γ-$BaAlF_5$, one can recognize the FeB-type structure (*10*) with quasi- no distortion; and finally, β-$BaAlF_5$ presents the SrAg-type structure (*11*). These similarities are detailed in Table VI. This means that, according to the well known discussion of twinning on the unit cell level as a structure-building operation (*12–14*), the stacking of the Ba cations is well described by

—twinned *ccp* Ba . . . , 1,1,1, . . . for α-$BaAlF_5$ (*c*),

—twinned *hcp* Ba . . . , 1,1,1, . . . for γ-$BaAlF_5$ (*h*), and

—twinned mixed (*h* and *c*)*cp* for β-$BaAlF_5$ (*hc*).

This description suggests a possible phase transition mechanism which is supported in Fig. 6.

Proposition of a Transitional Mechanism

As described by Parthé (*15*), the FeB-type structure can be developed by a shift from the CrB-type structure. The transition is known for some rare-earth silicides (see, for instance, (*16*)); however, it is reversible and no intermediate phase has been observed, although various CrB–FeB intergrowths are known (*14*). Here, the intermediate phase (β-$BaAlF_5$) shows the simplest *hc* stacking variant.

From the proposed topotactic transitional model of Fig. 6, relations between the cell parameters of the three phases can be proposed:

$$a_\beta \equiv c_\alpha$$

$$b_\beta \equiv 4b_\alpha - (a_\alpha + b_\alpha)/2 \quad \text{or} \equiv 4b_\alpha - (a_\alpha - b_\alpha)/2$$

$$c_\beta \equiv -(a_\alpha + b_\alpha)/2 \quad \text{or} \equiv -(a_\alpha - b_\alpha)/2$$

There are two orientational variants which could lead to microtwinning. For the $\beta \leftrightarrow \gamma$ transition, the relations are simpler and were given by Hoppe (1): $a_\gamma = a_\beta$; $b_\gamma = b_\beta/2$; $c_\gamma \equiv c_\beta$.

Several purely speculative points can be reasonably suggested, which are common to the two transitions:

—All the Al–F bonds are maintained during the transitions (i.e., the whole $(AlF_5)n$ chains undergo relative displacement from the other).

—Some Ba–F bonds must be broken and reconstructed after the shift of blocks noted *A* and *B* on Fig. 6. The main displacement occurs in the chain direction with a total shift of half the cell parameter in this direction (two adjacent blocks could displace 1/4 of ≈5 Å in opposite directions).

—In the plane perpendicular to the chain direction, the displacements in the non-*A*

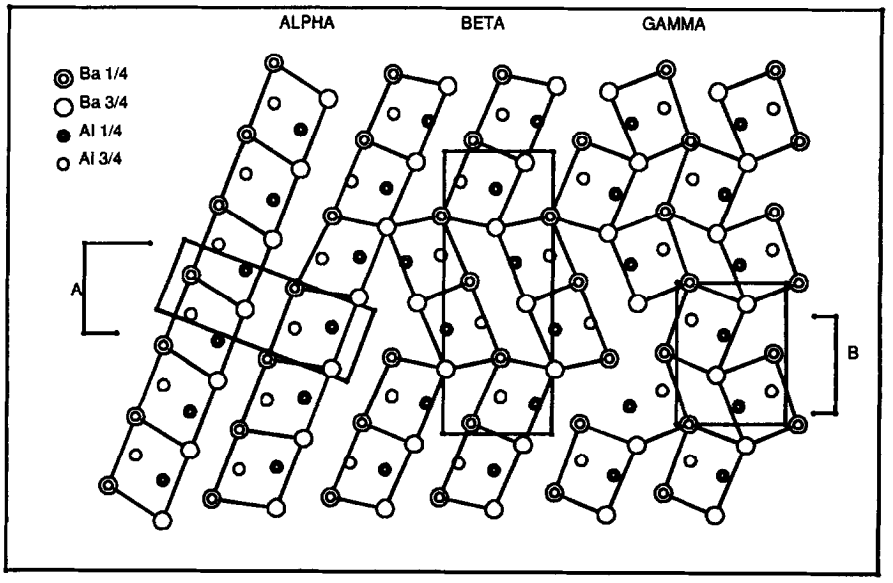

FIG. 6. The Ba–Al cationic subnetwork projected along [001] (α) or [100] (β- and γ-$BaAlF_5$). The coordinates along the projection axis are approximated and displaced by 1/4 for α and γ; other coordinates are exact. The *A* and *B* zones, on this speculative topotactic model, are the more perturbed during the transitions; they must undergo a shift of half the projection parameter and a shear parallel to the *c*-axis of the β and γ phases.

and non-*B* blocks are small, and they are less than 2 Å in the *A* and *B* blocks.

This model requires smaller displacements than the model of Parthé (*15*), which describes the CrB-type → FeB-type transition. When the latter is transposed to the $BaAlF_5$ case, it leads to the destruction of half the $(AlF_5)_n^{2n-}$ chains and to a shift of blocks of thickness b_γ, with an amplitude $c_\gamma/2$ (≈3.7 Å).

Finally, one can note that a group → subgroup relation is possible for the $\beta \leftrightarrow \gamma$ reversible transition but not for the $\alpha \rightarrow \beta$ irreversible transition.

Conclusion

Anionic or cationic subnetworks in more or less complicated structures are frequently found to mimic some basic simple structural types. The $BaAlF_5$ system seems to illustrate the transitions from twinned *ccp* (*c*) to twinned *hcp* (*h*) passing through the simplest intermediate state (*hc*). The parallelism is limited however, since the transition α-$BaAlF_5$ to β-$BaAlF_5$ is irreversible; furthermore a question arises about the role of pseudosymmetry in phase transitions.

Systematic twinning and/or fragmentation generally occurs during transitions, leading to the absence of single crystals suitable for structural purposes. We have contributed to demonstrate that such difficulty can be overcome by current methods of structure determination from powder data.

The $BaAlF_5$ system (which shows both reversible and irreversible transitions from acentric to centric space groups, related or unrelated, with a very low $\alpha \rightarrow \beta$ kinetic and a large hysteresis for $\beta \leftrightarrow \gamma$) offers a serious challenge to the physicists who wish to study it.

References

1. R. Domesle and R. Hoppe, *Z. Anorg. Allg. Chem.* **495,** 16 (1982).
2. R. Domesle and R. Hoppe, *Rev. Chim. Miner.* **15,** 439 (1978).
3. R. Domesle and R. hoppe, *Z. Anorg. Allg. Chem.* **495,** 27 (1982).
4. A. Le Bail, H. Duroy, and J. L. Fourquet, *Mat. Res. Bull.* **23,** 447 (1988).
5. G. Sheldrick, "SHELX: A Program for Crystal Structure Determination," University of Cambridge, England (1976).
6. "International Tables for X-ray Crystallography," Vol IV, Kynock Press, Birmingham (1974).
7. D. B. Wiles, A. Sakthivel, and R. A. Young, Program DBW3.2S (1987).
8. D. B. Wiles and R. A. Young, *J. Appl. Crystallogr.* **14,** 149 (1981).
9. R. Kiessling, *Acta Chem. Scand.* **3,** 595 (1949).
10. T. Bjurstrom, *Arkiv. Kemi Mineral. Geol.* **11A,** 12 (1933).
11. F. Merlo and M. L. Fornasini, *Acta Crystallogr. B* **37,** 500 (1981).
12. S. Andersson and B. G. Hyde, *J. Solid State Chem.* **9,** 92 (1974).
13. B. G. Hyde, A. N. Bagshaw, S. Andersson, and M. O'Keeffe, *Annu. Rev. Mater. Sci.* **4,** 43 (1974).
14. B. G. Hyde and S. Andersson (Eds.) "Inorganic Crystal Structures," Wiley, New York (1989).
15. E. Parthe, "Propriétés Thermodynamiques, Physiques, et Structurales des Dérivés Semi-métalliques," CNRS, Paris (1967).
16. D. Hohnke and E. Parthe, *Acta Crystallogr.* **20,** 572 (1966).